15

Particle Scale Simulation of Heat Transfer in Fluid Bed Reactors

Zongyan Zhou, Qinfu Hou and Aibing Yu
Laboratory for Simulation and Modelling of Particulate Systems School of Materials Science and Engineering, The University of New South Wales, Sydney, NSW 2052, Australia

1. Introduction

Fluid bed reactors have been extensively used in chemical processes due to their high heat transfer efficiency (Kunii & Levenspiel, 1991). Typical examples are ironmaking blast furnace which involves complicated multiphase flow, heat transfer and chemical reactions in a packed bed (Omori, 1987; Dong et al., 2007), and fluidized bed combustors whose performance heavily depends on the hydrodynamics and thermal-chemical behavior of particles in interaction with gas (Avedesia & Davidson, 1973; Oka, 2004). To achieve optimal design and control of such a fluid bed reactor, it is important to understand the flow and heat transfer characteristics. The thermal behaviour of packed beds with a stagnant or dynamic fluid has been extensively investigated experimentally and theoretically in the past decades. Many empirical correlations have been formulated to determine the heat transfer coefficient (HTC), as respectively reviewed by various investigators (Botterill, 1975; Wakao & Kaguei, 1982; Kunii & Levenspiel, 1991; Molerus & Wirth, 1997). Those studies and resulting formulations are mainly macroscopic, focused on the overall heat transfer behaviour. They are very useful to the estimation of the thermal behaviour of process designs.

Physical experiments usually experience difficulty in quantifying the heat transfer mechanisms at a particle level identified many years ago (for example, Yagi & Kunii, 1957). To overcome this difficulty, in recent years, heat transfer behaviour in a fluidized bed at a microscopic, particle scale has been examined experimentally (Prins et al., 1985; Baskakov et al., 1987; Agarwal, 1991; Parmar & Hayhurst, 2002; Collier et al., 2004; Scott et al., 2004). In such a study, the transient temperature of a hot sphere immersed in the bed is measured using an attached thermocouple, and then its HTC can be determined. Such particle scale studies are useful but have limitations in exploring the fundamentals. For example, the heat transfer to a particle should be described by at least three mechanisms, e.g. convection from fluid, conduction from particles or wall, and radiation. However, the contribution of each of these mechanisms is difficult to quantify. Moreover, the heat transfer of a particle will be strongly affected by the local gas-solid flow structure, and hence varies spatially and temporally. The information derived for a single particle may not be reliable because of the difficulty in quantifying such local structures in a particle bed.

Alternatively, mathematical modeling has been increasingly accepted as an effective method to study the heat transfer phenomena in a particle-fluid system. Generally speaking, the existing approaches to modelling particle flow and thermal behaviour can be classified into two categories: the continuum approach at a macroscopic level, and the discrete approach at a microscopic/particle level. In the continuum approach, the macroscopic behavior is described by balance equations, e.g., mass, momentum and energy, closed with constitutive relations together with initial and boundary conditions (see, for example, Anderson & Jackson, 1967; Ishii, 1975; Gidaspow, 1994; Enwald et al., 1996). The so called two-fluid model (TFM) is widely used in this approach. In such a model, both fluid and solid phases are treated as interpenetrating continuum media in a computational cell which is much larger than individual particles but still small compared with the size of process equipment (Anderson & Jackson, 1967). However, its effective use heavily depends on the constitutive or closure relations for the solid phase and the momentum exchange between phases which are often difficult to obtain within its framework.

The discrete approach is based on the analysis of the motion of individual particles, typically by means of the discrete particle simualtion (DPS). The method considers a finite number of discrete particles interacting by means of contact and non-contact forces. When coupling with fluid flow, a coupled DPS-CFD (computatinal fluid dynamics) approached is often used. In this approach, the motion of discrete particles is obtained by solving Newton's second law of motion, and the flow of continuum fluid by solving the Navier-Stokes equations based on the concept of local average as used in CFD, with the coupling of CFD and DPS through particle-fluid interaction forces (Tsuji et al., 1992; Xu & Yu, 1997; 1998; Zhou et al., 2010b). The main advantage of DPS-CFD is that it can generate detailed particle-scale information, such as the trajectories of and forces acting on individual particles, which is key to elucidating the mechanisms governing the complicated flow behavior. With the rapid development of computer technology, the approach has been increasingly used by various investigators to study various particle-fluid flow systems as, for example, reviewed by Zhu *et al.* (2007; 2008).

Discrete approach has been extended to study heat transfer. In fact, mechanistic approach based on the packet model originally proposed by Mickley and Fairbanks (1955) is a typical one to study the heat transfer between bubbling beds and immersed objects. However, the problem associated with such early approaches is the lack of reliable estimation of parameters (Chen, 2003; Chen et al., 2005). This difficulty can be overcome by the newly developed discrete approach. With the DPS-CFD approach, information such as particle-particle or particle-wall contact, local voidage and local gas-solid flow structure can be produced. Such information is essential in determining the heat transfer behaviour of individual particles. The approach has been attempted by some investigators to study coal combustion (Rong & Horio, 1999; Peters, 2002; Zhou et al., 2003; Zhou et al., 2004), air drying (Li & Mason, 2000; Li & Mason, 2002), olefin polymerization (Kaneko et al., 1999), and inserts in a fluidized bed (Di Maio et al., 2009; Zhao et al., 2009). But in those studies, the heat transfer mode by particle-particle conduction is only partially considered. The analysis of heat transfer mechanisms has not been performed seriously.

More recently, Zhou et al. (2009; 2010a) proposed a comprehensive model taking into account most of the known heat transfer mechanisms. The approach considers the different heat transfer mechanisms in detail, for example, particle-fluid convection, particle-particle

conduction, and particle radiation. The extended DPS-CFD model offers a useful numerical technique to elucidate the fundamentals governing the heat transfer in packed/fluidized beds at a particle scale. This chapter aims to introduce this approach, and demonstrates its applications through some case studies.

2. Model description

2.1 Governing equations for solid particles

Various methods have been developed for DPS simulation, as reviewed by Zhu et al. (2007). The DPS model used here is based on the soft sphere model, i.e. discrete element method (DEM), originally proposed by Cundall and Strack (1979). Generally, a particle in a particle-fluid flow system can have two types of motion: translational and rotational, which are determined by Newton's second law of motion. The corresponding governing equations for particle i with radius R_i, mass m_i and moment of inertia I_i can be written as:

$$m_i \frac{d\mathrm{v}_i}{dt} = \mathrm{f}_{f,i} + \sum_{j=1}^{k_c} (\mathrm{f}_{c,ij} + \mathrm{f}_{d,ij}) + m_i \mathrm{g} \tag{1}$$

$$I_i \frac{d\omega_i}{dt} = \sum_{j=1}^{k_c} (\mathrm{M}_{t,ij} + \mathrm{M}_{r,ij}) \tag{2}$$

where $\mathbf{v}_i$ and $\boldsymbol{\omega}_i$ are respectively the translational and angular velocities of the particle. The forces involved are: particle-fluid interaction force $\mathbf{f}_{f,i}$, the gravitational force $m_i\mathbf{g}$, and inter-particle forces between particles which include elastic force $\mathbf{f}_{c,ij}$ and viscous damping force $\mathbf{f}_{d,ij}$. These inter-particle forces can be resolved into the normal and tangential components at a contact point. The torque acting on particle i by particle j includes two components: $\mathbf{M}_{t,ij}$ which is generated by tangential force and causes particle i to rotate, and $\mathbf{M}_{r,ij}$ commonly known as the rolling friction torque, is generated by asymmetric normal forces and slows down the relative rotation between particles. A particle may undergo multiple interactions, so the individual interaction forces and torques are summed over the k_c particles interacting with particle i.

Equations used to calculate the interaction forces and torques between two spheres have been well-established in the literature (Zhu et al., 2007). In our work, the determination of particle-particle interaction is based on the non-linear models, as listed in Table 1. This approach was also used by other investigators (Langston et al., 1994; 1995; Zhou et al., 1999; Yang et al., 2000). Particle-fluid interaction force $\mathbf{f}_{f,i}$ is a sum of fluid drag $\mathbf{f}_{d,i}$ and pressure gradient force $\mathbf{f}_{\nabla p,i}$. Many correlations are available in the literature to calculate the fluid drag acting on the individual particles, for example, Ergun equation (1952), Wen and Yu (1966), and Di Felice (1994). Particularly, Di Felice correlation (1994) has been widely used in the literature and also used in our work (see, for example, Xu & Yu, 1997; Xu et al., 2000; Feng & Yu, 2004; 2007; Zhou et al., 2009; 2010a; 2010b).

The heat transfer of particle i and its surroundings is considered to be controlled by three mechanisms: particle-fluid convection, particle-particle or particle-wall conduction, and radiation. According to the energy balance, the governing equation for particle i can be generally written as

$$m_i c_{p,i} \frac{dT_i}{dt} = \sum_{j=1}^{k_i} Q_{i,j} + Q_{i,f} + Q_{i,rad} + Q_{i,wall} \tag{3}$$

where k_i is the number of particles exchanging heat with particle i, $Q_{i,j}$ is the heat exchange rate between particles i and j due to conduction, $Q_{i,f}$ is the heat exchange rate between particle i and its local surrounding fluid, $Q_{i,rad}$ is the heat exchange rate between particle i and its surrounding environment by radiation, and $Q_{i,wall}$ is particle-wall heat exchange rate. $c_{p,i}$ is the particle specific heat. Different heat transfer models are adopted to determine the different heat exchange rates shown in Eq. (3), and described below.

Normal elastic force, $\mathbf{f}_{\mathrm{cn,ij}}$	$-\frac{4}{3}E^*\sqrt{R^*}\delta_n^{3/2}\mathrm{n}$
Normal damping force, $\mathbf{f}_{\mathrm{dn,ij}}$	$-c_n\left(8m_{ij}E^*\sqrt{R^*\delta_n}\right)^{1/2}\mathrm{v}_{n,ij}$
Tangential elastic force, $\mathbf{f}_{\mathrm{ct,ij}}$	$-\mu_s\left\|\mathbf{f}_{cn,ij}\right\|(1-(1-\delta_t/\delta_{t,\max})^{3/2})\hat{\boldsymbol{\delta}}_t$
Tangential damping force, $\mathbf{f}_{\mathrm{dt,ij}}$	$-c_t\left(6\mu_s m_{ij}\left\|\mathbf{f}_{cn,ij}\right\|\sqrt{1-\delta_t/\delta_{t,\max}}/\delta_{t,\max}\right)^{1/2}\mathrm{v}_{t,ij}$
Coulomb friction force, $\mathbf{f}_{\mathrm{t,ij}}$	$-\mu_s\left\|\mathbf{f}_{cn,ij}\right\|\hat{\boldsymbol{\delta}}_t$
Torque by tangential forces, $\mathbf{T}_{\mathrm{t,ij}}$	$\mathrm{R}_{ij}\times\left(\mathbf{f}_{ct,ij}+\mathbf{f}_{dt,ij}\right)$
Rolling friction torque, $\mathbf{T}_{\mathrm{r,ij}}$	$\mu_{r,ij}\left\|\mathbf{f}_{n,ij}\right\|\hat{\boldsymbol{\omega}}_{ij}^n$
Particle-fluid drag force, $\mathbf{f}_{\mathrm{d,i}}$	$0.125C_{d0,i}\rho_f\pi d_{pi}^2\varepsilon_i^2\left\|\mathrm{u}_i-\mathrm{v}_i\right\|(\mathrm{u}_i-\mathrm{v}_i)\varepsilon_i^{-\chi}$
Pressure gradient force, $\mathbf{f}_{\nabla\mathrm{p,i}}$	$-V_{p,i}\nabla P_{d,i}$

where $1/m_{ij}=1/m_i+1/m_j$, $1/R^*=1/\left|\mathrm{R}_i\right|+1/\left|\mathrm{R}_j\right|$, $E^*=E/2(1-v^2)$,

$\hat{\boldsymbol{\omega}}_{ij}^n=\boldsymbol{\omega}_{ij}^n/\left|\boldsymbol{\omega}_{ij}^n\right|$, $\hat{\boldsymbol{\delta}}_t=\boldsymbol{\delta}_t/\left|\boldsymbol{\delta}_t\right|$, $\delta_{t,\max}=\mu_s\delta_n(2-v)/(2(1-v))$,

$\mathrm{v}_{ij}=\mathrm{v}_j-\mathrm{v}_i+\omega_j\times\mathrm{R}_j-\omega_i\times\mathrm{R}_i$, $\mathrm{v}_{n,ij}=(\mathrm{v}_{ij}\cdot\mathrm{n})\cdot\mathrm{n}$, $\mathrm{v}_{t,ij}=(\mathrm{v}_{ij}\times\mathrm{n})\times\mathrm{n}$,

$\chi=3.7-0.65\exp[-(1.5-\log_{10}\mathrm{Re}_i)^2/2]$, $C_{d0,i}=(0.63+4.8/\mathrm{Re}_i^{0.5})^2$,

$\mathrm{Re}_i=\rho_f d_{pi}\varepsilon_i\left|\mathbf{u}_i-\mathbf{v}_i\right|/\mu_f$.

Note that tangential forces ($\mathbf{f}_{\mathrm{ct,ij}}+\mathbf{f}_{\mathrm{dt,ij}}$) should be replaced by $\mathbf{f}_{\mathrm{t,ij}}$ when $\delta_t \geq \delta_{t,max}$.

Table 1. Components of forces and torques on particle i

Convective heat transfer

Convective heat transfer between particles and fluid has been extensively investigated since 1950s, and different equations have been proposed (Botterill, 1975; Wakao & Kaguei, 1982; Kunii & Levenspiel, 1991; Molerus & Wirth, 1997). Often, the convective heat transfer rate between particle i and fluid is calculated according to $Q_{i,f}=h_{i,conv}\cdot A_i\cdot(T_{f,i}-T_i)$, where A_i is the particle surface area, $T_{f,i}$ is fluid temperature in a computational cell where particle i is located, and $h_{i,conv}$ is the convective HTC. $h_{i,conv}$ is associated with the Nusselt number, which is a function of particle Reynolds number and gas Prandtl number, given by

$$Nu_i = h_{i,conv} d_{pi} / k_f = 2.0 + a \mathrm{Re}_i^b \mathrm{Pr}^{1/3} \quad (4)$$

where k_f and d_{pi} are the fluid thermal conductivity and particle diameter, respectively. Re_i is the local relative Reynolds number for particle i (Table 1). The gas (air) Prandtl number, Pr, is a material property. The constant, 2.0, represents the contribution by particle-fluid natural convection. a and b are two parameters that need to be evaluated. As suggested by Kunii and Levenspiel (1991), b=0.5, and a could range from 0.6 to 1.8, depending on the bed conditions.

For fluid-wall heat transfer, $Nu_D = h_{f,wall} D / k_f = 0.023 \mathrm{Re}^{0.8} \mathrm{Pr}^n$ is used to determine the heat transfer coefficient $h_{f,wall}$, where D is the hydraulic diameter, and the exponent n is 0.4 for heating, and 0.3 for cooling (Holman, 1981).

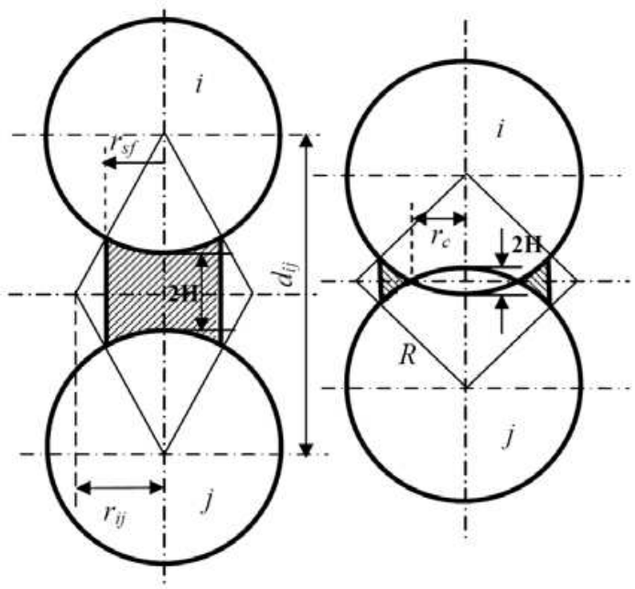

(a) (b)

Fig. 1. Schematic of the relative positions of two spheres: (a) non-contact; and (b) contact with an overlap (Zhou et al., 2009)

Conductive heat transfer

Conduction between particles involves various mechanisms (Yagi & Kunii, 1957; Cheng et al., 1999), which mainly include (i) particle-fluid-particle conduction heat transfer; and (ii) particle-particle conduction heat transfer, as indicated in Fig. 1. The model details for those two mechanisms are described as follows.

Particle-fluid-particle heat transfer has been examined by various investigators (Delvosalle & Vanderschuren, 1985; Cheng et al., 1999). The model proposed by Cheng et al. (1999) is used here after some modification. According to this model, the heat transfer flux between spheres i and j is written as

$$Q_{i,j} = (T_j - T_i) \int_{r_{sij}}^{r_{sf}} \frac{2\pi \cdot r dr}{(\sqrt{R^2 - r^2} - r(R+H)/r_{ij}) \cdot \left(1/k_{pi} + 1/k_{pj}\right) + 2[(R+H) - \sqrt{R^2 - r^2}]/k_f} \quad (5)$$

where k_{pi} and k_{pj} are the thermal conductivities of particles i and j, respectively. For the details of parameters of H, r_{sf} and r_{ij}, see the reference of Zhou et al. (2009). The heat flux between two particles is ignored when the distance of 2H is greater than particle radius R.

Conduction heat transfer always occurs through the contacted area between particles or between particles and wall. Generally, such conduction heat transfer due to elastic deformation includes two mechanisms: conduction due to particle-particle static contact (particularly common in a packed bed) and conduction due to particle-particle collision, which occurs in a moving or fluidized bed. For conduction due to particle-particle static contact, the equation proposed by Batchelor and O'Brien (Batchelor & O'Brien, 1977) and modified by Cheng et al. (1999) is adopted. Thus, the heat flux $Q_{i,j}$ through the contact area between particles i and j can be calculated according to the equation below:

$$Q_{i,j} = \frac{4r_c(T_j - T_i)}{(1/k_{pi} + 1/k_{pj})} \tag{6}$$

Particle-particle heat transfer due to collision is normally determined by the model proposed by Sun and Chen (1988). Recently, Zhou et al. (2008) provided a modified equation that can be readily implemented in the DPS-CFD model:

$$Q_{i,j} = c' \frac{(T_j - T_i)\pi \ r_c^2 t_c^{-1/2}}{(\rho_{pi} c_{pi} k_{pi})^{-1/2} + (\rho_{pj} c_{pj} k_{pj})^{-1/2}} \tag{7}$$

where r_c and t_c are particle-particle contact radius and contact duration, respectively. To be consistent with the current model, r_c is obtained from the DEM simulation which is based on the Hertz elastic contact theory (see Table 1). For particle-wall static or collision contact, a wall can be treated as a particle with an infinite diameter and mass, as commonly used in the DEM work. Its properties are assumed to be the same as particles.

It should be noted that the two mechanisms represented by Eqs. (6) and (7) must be distinguished in computation (Zhou et al., 2009). For fixed beds, particle-particle contacts are all static. Thus only static contact heat transfer applies. For fluidized beds, two parameters are set: particle-particle collision time t_c, and particle-particle contact duration time t_d which can be obtained from simulation. For two colliding particles, if $t_c \geq t_d$, only collisional heat transfer applies. If $t_c < t_d$, two particles will keep in touch after collision. In such a case, collision heat transfer applies first during the time of t_c, and then static heat transfer during the time of $(t_d - t_c)$.

Radiative heat transfer

In a fixed or fluidized bed, a particle is surrounded by particles and fluid. In a specified enclosed cell, an environmental temperature is assumed to represent the enclosed surface temperature around such a particle. Thus, the equation used by Zhou et al. (2004) is slightly modified to calculate the heat flux due to radiation using a local environmental temperature to replace the bed temperature, and is written as (Zhou et al., 2009)

$$Q_{i,rad} = \sigma \varepsilon_{pi} A_i (T_{local,i}^4 - T_i^4) \tag{8}$$

where σ is the Stefan-Boltzmann constant, equal to 5.67×10^{-8} W/(m²·K⁴), and ε_{pi} is the sphere emissivity. Gas radiation is not considered due to low gas emissivities. The parameter $T_{local,i}$ is the averaged temperature of particles and fluid by volume fraction in a enclosed spherical domain Ω given by (Zhou et al., 2009)

$$T_{local,i} = \varepsilon_f T_{f,\Omega} + (1-\varepsilon_f)\frac{1}{k_\Omega}\sum_{j=1}^{k_\Omega} T_j (j \neq i) \tag{9}$$

where $T_{f,\Omega}$ and k_Ω are respectively the fluid temperature and the number of particles located in the domain Ω with its radius of $1.5d_p$. To be fully enclosed, a larger radius can be used.

2.2 Governing equations for fluid phase

The continuum fluid field is calculated from the continuity and Navier-Stokes equations based on the local mean variables over a computational cell, which can be written as (Xu et al., 2000)

$$\frac{\partial \varepsilon_f}{\partial t} + \nabla \cdot (\varepsilon_f \mathbf{u}) = 0 \tag{10}$$

$$\frac{\partial (\rho_f \varepsilon_f \mathbf{u})}{\partial t} + \nabla \cdot (\rho_f \varepsilon_f \mathbf{u}\mathbf{u}) = -\nabla p - \mathbf{F}_{fp} + \nabla \cdot \varepsilon_f \boldsymbol{\tau} + \rho_f \varepsilon_f \mathbf{g} \tag{11}$$

And by definition, the corresponding equation for heat transfer can be written as

$$\frac{\partial (\rho_f \varepsilon_f c_p T)}{\partial t} + \nabla \cdot (\rho_f \varepsilon_f \mathbf{u} c_p T) = \nabla \cdot (c_p \Gamma \nabla T) + \sum_{i=1}^{k_V} Q_{f,i} + Q_{f,wall} \tag{12}$$

where $\mathbf{u}$, ρ_f, p and $\mathbf{F}_{fp}(=(\sum_{i=1}^{k_V}\mathbf{f}_{f,i})/\Delta V))$ are the fluid velocity, density, pressure and volumetric fluid-particle interaction force, respectively, and k_V is the number of particles in a computational cell of volume ΔV. Γ is the fluid thermal diffusivity, defined by μ_e/σ_T, and σ_T the turbulence Prandtl number. $Q_{f,i}$ is the heat exchange rate between fluid and particle i which locates in a computational cell, and $Q_{f,wall}$ is the fluid-wall heat exchange rate. $\boldsymbol{\tau}$ $(=\mu_e[(\nabla \mathbf{u}) + (\nabla \mathbf{u})^{-1}])$ and ε_f $(=(1-(\sum_{i=1}^{k_V} V_{p,i})/\Delta V)$ are the fluid viscous stress tensor and porosity, respectively. $V_{p,i}$ is the volume of particle i (or part of the volume if the particle is not fully in the cell), μ_e the fluid effective viscosity determined by the standard k-ε turbulent model (Launder & Spalding, 1974).

2.3 Solutions and coupling schemes

The methods for numerical solution of DPS and CFD have been well established in the literature. For the DPS model, an explicit time integration method is used to solve the translational and rotational motions of discrete particles (Cundall & Strack, 1979). For the CFD model, the conventional SIMPLE method is used to solve the governing equations for the fluid phase (Patankar, 1980). The modelling of the solid flow by DPS is at the individual particle level, whilst the fluid flow by CFD is at the computational cell level. The coupling methodology of the two models at different length scales has been well documented (Xu & Yu, 1997; Feng & Yu, 2004; Zhu et al., 2007; Zhou et al., 2010b). The present model simply

extends that approach to include heat transfer, and more details can be seen in the reference of Zhou et al. (2009).

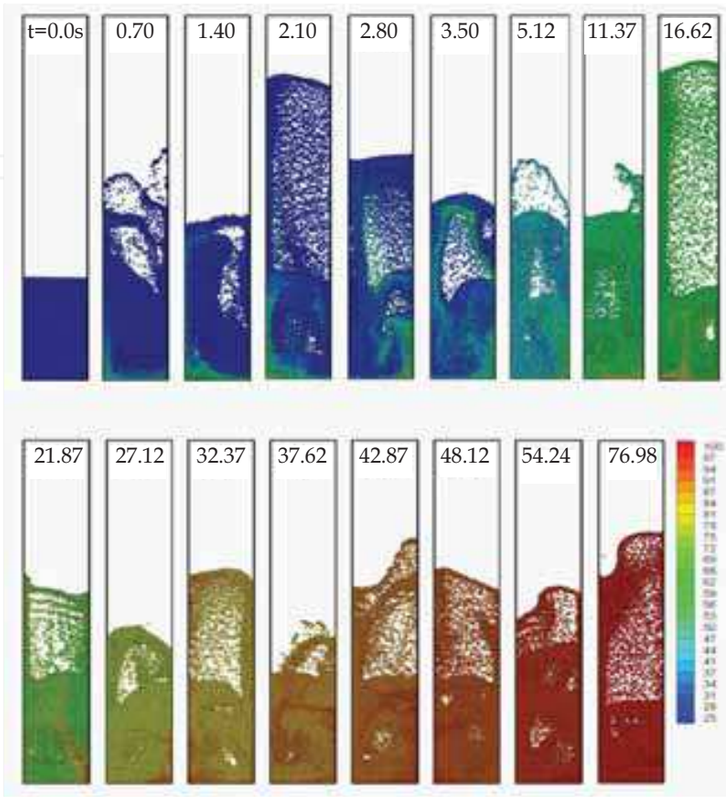

Fig. 2. Snapshots showing the heating process of fluidized bed by hot gas (1.2 m/s, 100°C) uniformly introduced from the bottom (Zhou et al., 2009).

3. Model application

3.1 Heat transfer in gas fluidization with non-cohesive particles

Gas fluidization is an operation by which solid particles are transformed into a fluid-like state through suspension in a gas (Kunii & Levenspiel, 1991). By varying gas velocity, different flow patterns can be generated from a fixed bed ($U<U_{mf}$) to a fluidzied bed. The solid flow patterns in a fluidized bed are transient and vary with time, as shown in Fig. 2, which also illustrates the variation of particle temperature. Particles located at the bottom are heated first, and flow upward dragged by gas. Particles with low temperatures descend and fill the space left by those hot particles. Due to the strong mixing and high gas-particle heat transfer rate, the whole bed is heated quickly, and reaches the gas inlet temperature at around 70 s. The general features observed are qualitatively in good agreement with those reported in the literature, confirming the predictability of the proposed DPS-CFD model in dealing with the gas-solid flow and heat transfer in gas fluidization.

The cooling of copper spheres at different initial locations in a gas fluidzied bed was examined by the model (Zhou et al., 2009). In physical experiments, the temperature of hot spheres is measured using thermocouples connected to the spheres (Collier et al., 2004; Scott

et al., 2004). But the cooling process of such hot spheres can be easily traced and recorded in the DPS-CFD simulations, as shown in Fig. 3a. The predicted temperature is comparable with the measured one. The cooling curves of 9 hot spheres are slightly different due to their different local fluid flow and particle structures. In the fixed bed, such a difference is mainly contributed to the difference in the local structures surrounding the hot sphere. But in the fluidized bed, it is mainly contributed to the transient local structure and particle-particle contacts or collisions. Those factors determine the variation of the time-averaged HTCs of hot spheres in a fluidized bed.

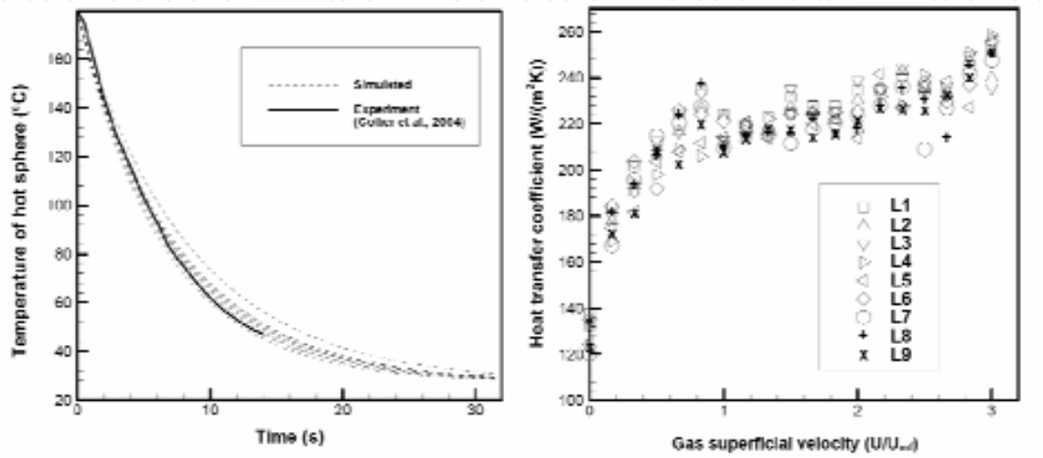

a) b)

Fig. 3. (a) Temperature evolution of 9 hot spheres when gas superficial velocity is 0.42 m/s; and (b) time-averaged heat transfer coefficients of the 9 hot spheres as a function of gas superficial velocity (Zhou et al., 2009).

The comparison of the HTC-U relationship between the simulated and the measured was made (Zhou et al., 2009). In physical experiments, Collier et al. (2004) and Scott et al. (2004) used different materials to examine the HTCs of hot spheres, and found that there is a general tendencyfor the HTC of hot sphere increasing first with gas superficial velocity in the fixed bed ($U<U_{mf}$), and then remaining constant, independent on the gas superficial velocities for fluidized beds ($U>U_{mf}$). The DPS-CFD simulation results also exhibit such a feature (Fig. 3b). For packed beds, the time-averaged HTC increases with gas superficial velocity, and reaches its maximum at around $U=U_{mf}$. After the bed is fluidized, the HTC is almost constant in a large range.

The HTC-U relationship is affected significantly by the thermal conductivity of bed particles (Zhou et al., 2009). The higher the k_p, the higher the HTC of hot spheres (Fig. 4). For exmaple, when k_p=30 W/(m·K), the predicted HTC in the fixed bed ($U/U_{mf}<1$) is so high that the trend of HTC-U relationship shown in Fig. 3b is totally changed. The HTC decreases with U in the fixed bed, then may reach a constant HTC in the fluidized bed. But when thermal conductivity of particles is low, the HTC always increases with U, independent of bed state (Fig. 4a). Fig. 4b further explains the variation trend of HTC with U. Generally, the convective HTC increases with U; but conductive HTC decreases with U. For a proper particle thermal conductivity, i.e. 0.84 W/(m·K), the two contributions (convective HTC and conductive HTC) could compensate each other, then the total HTC is nearly constant after

the bed is fluidized. So HTC independence of U is valid under this condition. But if particle thermal conductivity is too low or too high, the relationship of HTC and U can be different, as illustrated in Fig. 4a.

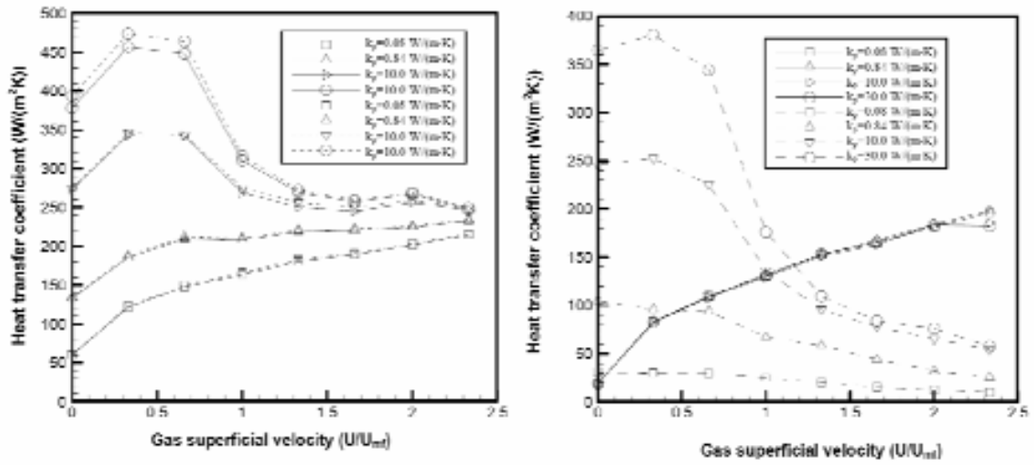

a) b)

Fig. 4. Time-averaged heat transfer coefficients of one hot sphere: (a) total HTC calculated by different equations; and (b) convective HTC (solid line) and conductive HTC (dashed line) for different thermal conductivities (Zhou et al., 2009).

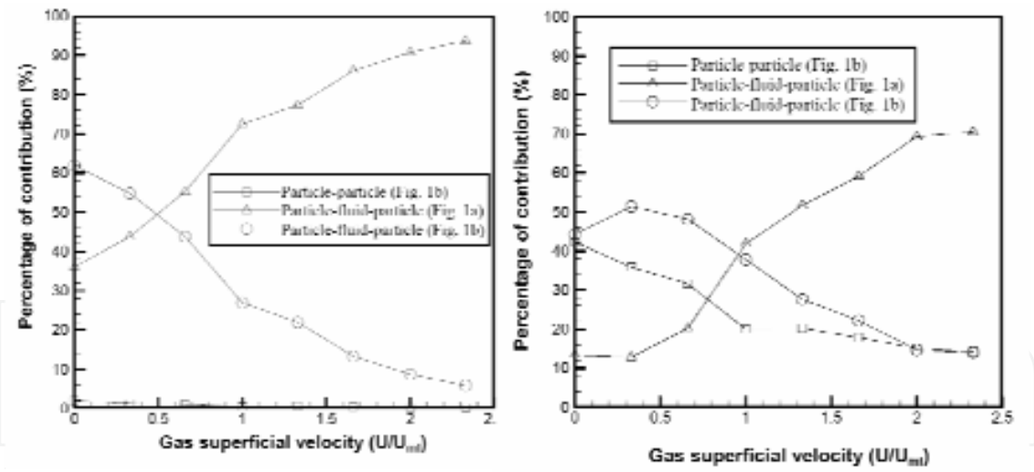

a) b)

Fig. 5. Contributions to conduction heat transfer by different heat transfer mechanisms when (a) k_p=0.08 W/(m·K); and (b) k_p=30 W/(m·K) (Zhou et al., 2009).

The proposed DPS-CFD model can be used to analyze the sub-mechanisms shown in Fig. 1a for conduction. The relative contributions by these heat transfer paths were quantified (Zhou et al., 2009). For example, when k_p=0.08 W/(m·K), particle-fluid-particle conduction always contributes more than particle-particle contact, but both vary with gas superficial velocity (Fig. 5a). For particle-fluid-particle conduction, particle-fluid-particle heat transfer with two contacting particles is far more important than that with two non-contacting

particles in the fixed bed. Zhou et al. (2009) explained that it is because the hot sphere contacts about 6 particles when $U<U_{mf}$. But such a feature changes in the fluidized bed ($U>U_{mf}$), where particle-fluid-particle conduction between non-contacting particles is relatively more important. This is because most of particle-particle contacts with an overlap are gradually destroyed with increasing gas superficial velocity, which significantly reduces the contribution by particle-fluid-particle between two contacting particles. However, particle-particle conduction through the contacting area becomes more important with an increase of particle thermal conductivity. The percentage of its contribution is up to 42% in the fixed bed when k_p=30 W/(m·K), then reduces to around 15% in the fluidized bed (Fig. 5b). Correspondingly, the contribution percentage by particle-fluid-particle heat transfer is lower, but the trend of variation with U is similar to that for k_p=0.08 W/(m·K).

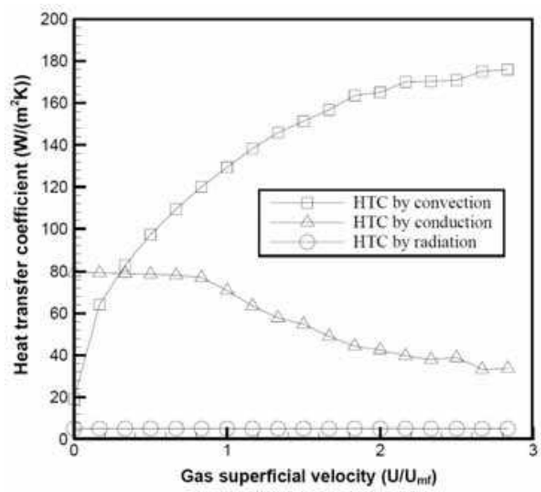

Fig. 6. Bed-averaged convective, conductive and radiative heat transfer coefficients as a function of gas superficial velocity (Zhou et al., 2009).

It should be noted that a fluid bed has many particles. A limited number of hot spheres cannot fully represent the averaged thermal behaviour of all particles in a bed. Thus, Zhou et al. (2009) further examined the HTCs of all the particles, and found that the features are similar to those observed for hot spheres (Fig. 6). The similarity illustrates that the hot sphere approach can, at least partially, represent the general features of particle thermal behaviour in a particle-fluid bed. Overall, the particles in a uniformly fluidized bed behave similarly. But a particle may behave differently from another at a given time. Zhou et al. (2009) examined the probability density distributions of time-averaged HTCs due to particle-fluid convection and particle conduction, respectively (Fig. 7). The convective HTC in the packed bed varies in a small range due to the stable particle structure. Then the distribution curve moves to the right as U increases, indicating the increase of convective HTC. The distribution curve also becomes wider. It is explained that, in a fluidized bed, clusters and bubbles can be formed, and the local flow structures surrounding particles vary in a large range. The density distribution of time-averaged HTCs by conduction shows that it has a wider distribution in a fixed bed (curves 1, 2 and 3) (Fig. 7b), indicating different local packing structures of particles. But curves 1 and 2 are similar. It is explained that, statistically, the two bed packing structures are similar, and do not vary much even if U is different. When $U>U_{mf}$ (e.g. $U=2.0U_{mf}$), the distribution curve moves to the left, indicating

the heat transfer due to interparticle conduction is reduced. The bed particles occasionally collide and contact each other. Statistically, the number of collisions and contacts are similar in fully fluidized beds, and not affected significantly by gas superficial velocities. Those features are consistent with those observed using the hot sphere approach. It confirms that hot sphere approach can represent the thermal behaviour of all bed particles to some degree.

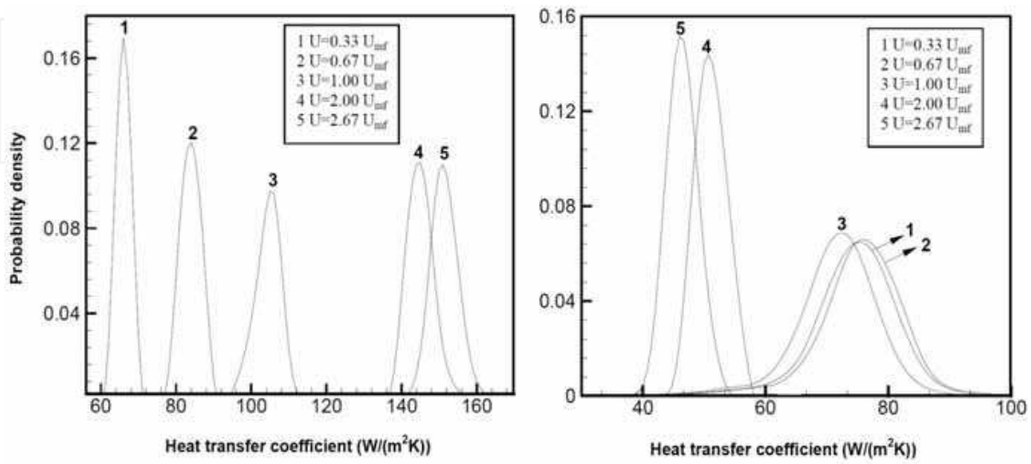

Fig. 7. Probability density distributions of time-averaged heat transfer coefficients of particles at different gas superficial velocities: (a), fluid convection; and (b), particle conduction (Zhou et al., 2009).

The particle thermal behaviour in a fluidized bed is affected by bed temperature. Zhou et al. (2009) carried out a simulation case at high tempertaure of 1000°C. It illustrated that the radiative HTC reaches 300 W/(m²·K), which is significantly larger than that for the case of hot gas with 100°C (around 5 W/(m²·K). The convective and radiative HTCs do not remain constant during the bed heating due to the variation of gas properties with temperature. The conductive heat transfer coefficient is not affected much by the bed temperature. This is because the conductive HTC is quite small in the fluidized bed, and only related to the gas and particle thermal conductivities.

3.2 Effective thermal conductivity in a packed bed.

Effective thermal conductivity (ETC) is an important parameter describing the thermal behaviour of packed beds with a stagnant or dynamic fluid, and has been extensively investigated experimentally and theoretically in the past. Various mathematical models, including continuum models and microscopic models, have been proposed to help solve this problem, but they are often limited by the homogeneity assumption in a continuum model (Zehner & Schlünder, 1970; Wakao & Kaguei, 1982) or the simple assumptions in a microscopic model (Kobayashi et al., 1991; Argento & Bouvard, 1996). Cheng et al. (1999; 2003) proposed a structure-based approach, and successfully predicted the ETC and analyzed the heat transfer mechanisms in a packed bed with stagnant fluid. Such efforts have also been made by other investigators (Vargas & McCarthy, 2001; Vargas & McCarthy, 2002a; b; Cheng, 2003; Siu & Lee, 2004; Feng et al., 2008). The proposed structured-based approach has been extended to account for the major heat transfer mechanisms in the calculation of ETC of a packed bed with a stagnant fluid (Cheng, 2003). But it is not so

adaptable or general due to the complexity in the determination of the packing structure and the ignorance of fluid flow in a packed bed. The proposed DPS-CFD model has shown a promising advantage in predicting the ETC under the different conditions (Zhou et al., 2009; 2010a).

Crane and Vachon (1977) summarized the experimental data in the literature, and some of them were further collected by Cheng et al. (1999) to validate their structure-based model (for example, see data from (Kannuluik & Martin, 1933; Schumann & Voss, 1934; Waddams, 1944; Wilhelm et al., 1948; Verschoor & Schuit, 1951; Preston, 1957; Yagi & Kunii, 1957; Gorring & Churchill, 1961; Krupiczka, 1967; Fountain & West, 1970)). Our work makes use of their collected data. In the structure-based approach (Cheng et al., 1999), it is confirmed that the ETC calculation is independent of the cube size sampled from a packed bed when each cube side is greater than 8 particle diameters. Zhou et al. (2009; 2010a) gave the details on how to determine the bed ETC. The size of the generated packed bed used is $13d_p \times 13d_p \times 16d_p$. 2,500 particles with diameter 2 mm and density 1000 kg/m^3 are packed to form a bed by gravity. Then the ETC of the bed is determined by the following method: the temperatures at the bed bottom and top are set constants, T_b=125°C and T_t=25°C, respectively. Then a uniform heat flux, q (W/m^2), is generated and passes from the bottom to the top. The side faces are assumed to be adiabatic to produce the un-directional heat flux. Thus, the bed ETC is calculated by $k_e = q \cdot H_b / (T_b - T_t)$, where H_b is the height between the two layers with two constant temperatures at the top and the bottom, respectively.

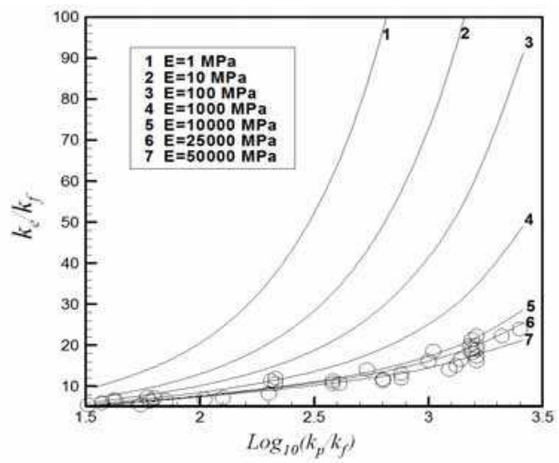

Fig. 8. Effect of Young's modulus E on the bed ETC (the experimental data represented by circles are from the collection of Cheng et al. (1999)) (Zhou et al., 2010a).

Young's modulus is an important parameter affecting the particle-particle overlap, hence the particle-particle heat transfer (Zhou et al., 2010a). Fig. 8 shows the predicted ETC for different Young's modulus varying from 1 MPa to 50 GPa. When E is around 50 GPa, which is in the range of real hard materials like glass beads, the predicted ETC are comparable with experiments. The high ETC for low Young's modulus is caused by the overestimated particle-particle overlap in the DPS based on the soft-sphere approach. A large overlap significantly increases the heat flux Q_{ij}. However, in the DPS, it is computationally very demanding to carry out the simulation using a real Young's modulus (often at an order of 10^3~10^5 MPa), particularly when involving a large number of particles. This is because a high Young's modulus requires extremely small time steps to obtain accurate results,

resulting in a high computational cost which may not be tolerated under the current computational capacity. The relationship often used for determining the time step is in the form of $\Delta t \propto \sqrt{m/k}$, where k is the particle stiffness. The higher the stiffness, the smaller the time step. It is therefore very helpful to have a method that can produce accurate results but does not have a high computational cost.

The calculation of heat fluxes for conduction heat transfer mechanisms is related to an important parameter: particle-particle contact radius r_c, as seen in Eqs. (6) and (7) Unfortunately, DPS simulation developed on the basis of soft-sphere approach usually overestimates r_c due to the use of low Young's modulus. The overestimation of r_c then significantly affects the calculation of conductive heat fluxes. To reduce such an over-prediction, a correction coefficient c is introduced, and then the particle-particle contact radius used to calculate the heat flux between particles through the contact area is written as

$$r_c{}' = c \cdot r_c \tag{13}$$

where r_c' is the reduced contact radius by correction coefficient c which varies between 0 and 1, depending on the magnitude of Young's modulus used in the DPS. The determination of c is based on the Hertzian theory, and can be written as (Zhou et al., 2010a)

$$c = r_{c,0}/r_c = (E_{ij}/E_{ij,0})^{1/5} \tag{14}$$

where $E_{ij} = 4/3[(1-\nu_i^2)/E_i + (1-\nu_j^2)/E_j]$, $E_{ij,0} = 4/3[(1-\nu_i^2)/E_{i,0} + (1-\nu_j^2)/E_{j,0}]$, ν is passion ratio, and E_i is the Young's modulus used in the DPS. It can be observed that, to determine the introduced correction coefficient c, two parameters are required: E_{ij}, the value of Young's modulus used in the DPS simulation and $E_{ij,0}$, the real value of Young's modulus of the materials considered. Different materials have different Young's modulus E_0. Then the obtained correction coefficients by Eq. (14) are also different, as shown in Fig. 9a. Fig. 9b further shows the applications of the otained correction coefficeints in some cases, where the particle thermal conductivity varied from 1.0 to 80 W/(m·K); gas thermal conductivities varied from 0.18 to 0.38 W/(m·K); Young's modulus used in the DPS varies from 1 MPa to 1 GPa, and the real value of Young's modulus is set to 50 GPa. The results show that the predicted ETCs are well comparable with experiments.

There are many factors influencing the ETC of a packed bed. The main factors are the thermal conductivities of the solid and fluid phases. Other factors include particle size, particle shape, packing method that gives different packing structures, bed temperature, fluid flow and other properties. Zhou et al. (2010a) examined the effects of some parameters on ETC, and revealed tha ETC is not sensitive to particle-particle sliding friction coefficient which varies from 0.1 to 0.8. ETC increases with the increase of bed average temperature, which is consistent with the observation in the literature (Wakao & Kaguei, 1982). The predicted ETC at 1475°C can be about 5 times larger than that at 75°C. The effect of particle size on ETC is more complicated. At low thermal conductivity ratios of k_p/k_f, the ETC varies little with particle size from 250 μm to 10 mm. But it is not the case for particles with high thermal conductivity ratios, where the ETC increases with particle size. The main reason could be that the particle-particle contact area is relatively large for large particles, and consequently, the increase of k_p/k_f enhances the conductive heat transfer between particles. However, that ETC is affected by particle size offers an explanation as to why the literature

data are so scattered. This is because different sized particles were used in experiments. For particles smaller than 500 μm, the predicted ETC is lower than that measured for high k_p/k_f ratios. This is because large particles were used in the reported experiments. Further studies are required to quantify the effect of particle size on the bed ETC under the complex conditions with moving fluid, size distributions or high bed temperature corresponding to those in experiments (Khraisha, 2002; Fjellerup et al., 2003; Moreira et al., 2005).

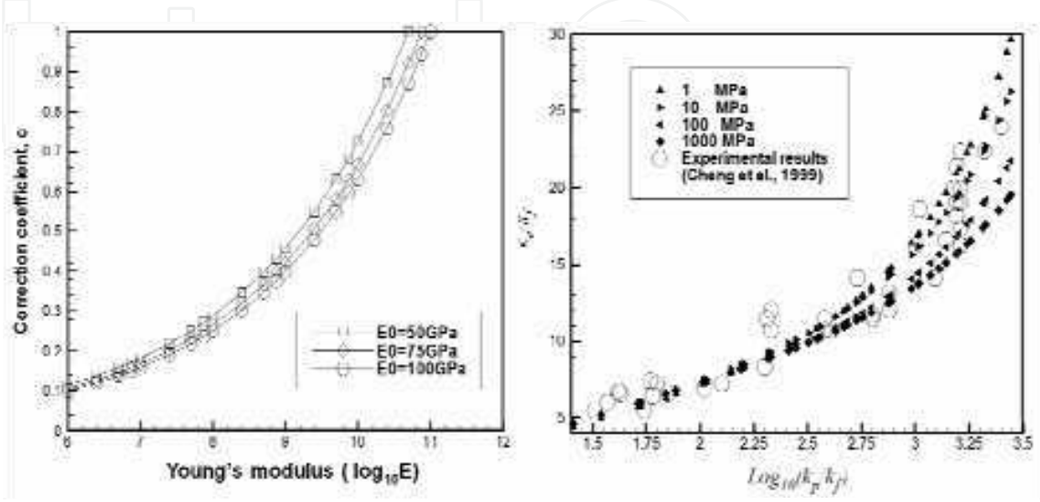

a) b)

Fig. 9. (a) Relationship between correction coefficient and Young's modulus E used in the DPS, and (b) the predicted ETCs as a function of k_p/k_f ratios for different E using the obtained correction coefficients according to Eq. (14) where E_0=50 GPa (Zhou et al., 2010a).

The approach of introduction of correction coefficient has also been applied to gas fluidization to test its applicability. An example of flow patterns has been shown in Fig. 2, which illustrates a heating process of the fluidized bed by hot gas (Zhou et al., 2009). The proposed modified model by an introduction of correction coefficient in this work can still reproduce those general features of solid flow patterns and temperature evolution with time using low Young's modulus, and the obtained results are comparable to those reported by Zhou et al. (2009) using a high Young's modulus. Zhou et al. (2010a) compared the obtained average convective and conductive heat transfer coefficients by three treatments: (1) $E=E_0$=50 GPa, and c=1.0; (2) E=10 MPa, and c=1.0; and (3) E=10 MPa, and c=0.182. Treatment 1 corresponds to the real materials, and its implementation requires a small time step. Treatments 2 and 3 reduce the Young's modulus so that a large time step is applicable. The difference between them is one with reduced contact radius (c=0.182 in treatment 3), and another not (c=1 in treatment 2). The results are shown in Fig. 10. The convective heat transfer coefficient is not affected by those treatments (Fig. 10a). Particle-particle contact only affects the conduction heat transfer (Fig. 10b). The results are very comparable and consistent between the models using treatments 1 and 3, but they are quite different from the model using the treatment 2. If the particle thermal conductivity is high, such difference becomes even more significant. The comparison in Fig. 10b indicates that the modified model by treatment 3 can be used in the study of heat transfer not only in packed beds but also in fluidization beds. It must be pointed out that the significance of proposed modified

model (treatment 3) is to save computational cost. For the current case shown in Fig. 10, the use of a low Young's modulus significantly reduces the computational time, i.e. 4~5 times faster with 16,000 particles. Such a reduction becomes more significant for a larger system involving a large number of particles.

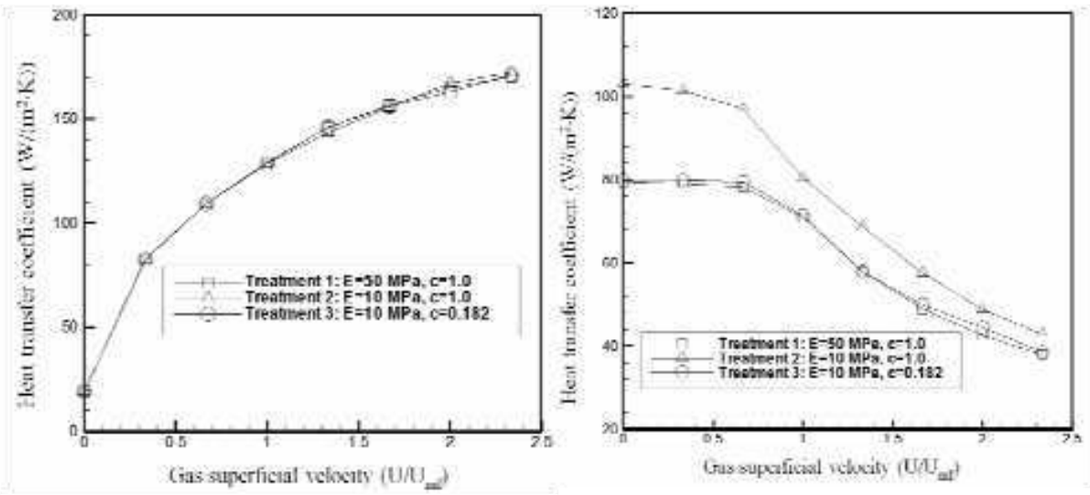

a) b)

Fig. 10. Average convective heat transfer coefficient (a) and conductive heat transfer coefficient (b) of bed particles with different gas superficial velocities (k_p=0.84 W/(m·K)).

3.3 Heat transfer between a fluidized bed and an insert tube

Immersed surfaces such as horizontal/vertical tubes, fins and water walls are usually adopted in a fluidized bed to control the heat addition or extraction (Chen, 1998). Understanding the flow and heat transfer mechanisms is important to achieve its optimal design and control (Chen et al., 2005). The relation of the HTC of a tube and gas-solid flow characteristic in the vicinity of the tube such as particle residence time and porosity has been investigated experimentally using heat-transfer probe and positron emission particle tracking (PEPT) method or an optical probe (Kim et al., 2003; Wong & Seville, 2006; Masoumifard et al., 2008). The variations of HTC with probe positions and inlet gas superficial velocity are interpreted mechanistically. The observed angular variation of HTC is explained by the PEPT data.

Alternatively, the DPS-CFD approach has been used to study the flow and heat transfer in fluidization with an immersed tube in the literature (Wong & Seville, 2006; Di Maio et al., 2009; Zhao et al., 2009). Di Maio et al. (2009) compared different particle-to-particle heat transfer models and suggested that the formulation of these models are important to obtain comparable results to the experimental measurements. Zhao et al. (2009) used the unstructured mesh which is suitable for complex geometry and discussed the effects of particle diameter and superficial gas velocity. They obtained comparable prediction of HTC with experimental results at a low temperature. These studies show the applicability of the proposed DPS-CFD approach to a fluidized bed with an immersed tube. However, some important aspects are not considered in these studies. Firstly, their work is two dimensional with the bed thickness of one particle diameter. But as laterly pointed out by Feng and Yu (2010), three dimensional bed is more reliable to investigate the structure related

phenomena such as heat transfer. Secondly, the fluid properties such as fluid density and thermal conductivity are considered as constants. However, the variations of these properties have significant effect on the heat transfer process (Botterill et al., 1982; Pattipati & Wen, 1982). Thirdly, although the particle-particle heat transfer has proved to be critical for generation of sound results (Di Maio et al., 2009), the heat transfer through direct particle contact in these works simply combined static and collisional contacts mechanisms together, which are two important mechanisms particularly in a dynamic fluidized bed (Sun & Chen, 1988; Zhou et al., 2009). Finally, the radiative heat transfer mechanism is ignored, which is significant in a fluidized bed at high temperatures (Chen & Chen, 1981; Flamant & Arnaud, 1984; Chung & Welty, 1989; Flamant et al., 1992; Chen et al., 2005).

Recently, Hou et al. (2010a; 2010b) used the proposed DPS-CFD model to investigate the heat transfer in gas fluidization with an immersed horizontal tube in a three dimensional bed. The simulation conditions are similar to the experimental investigations by Wong and Seville (2006) except for the bed geometry. The predicted result of 0.27 m/s for minimum fluidization velocity (u_{mf}) is consistent with those experimental measurements (Chandran & Chen, 1982; Wong & Seville, 2006). Fig. 11 shows the snapshots of flow patterns obtained from the DPS-CFD simulation. The bubbling fluidized bed behaviour is significantly affected by the horizontal tube. Two main features can be identified: defluidized region in the downstream and the air film in the upstream (Glass & Harrison, 1964; Rong et al., 1999; Wong & Seville, 2006). Particles with small velocities tend to stay on the tube in the downstream and form the defluidized region intermittently. The thickness of the air film below the tube changes with time. There is no air film and the upstream section is fully filled with particles at some time intervals (e.g. t = 1.3 s and 3.0 s in Fig. 11).

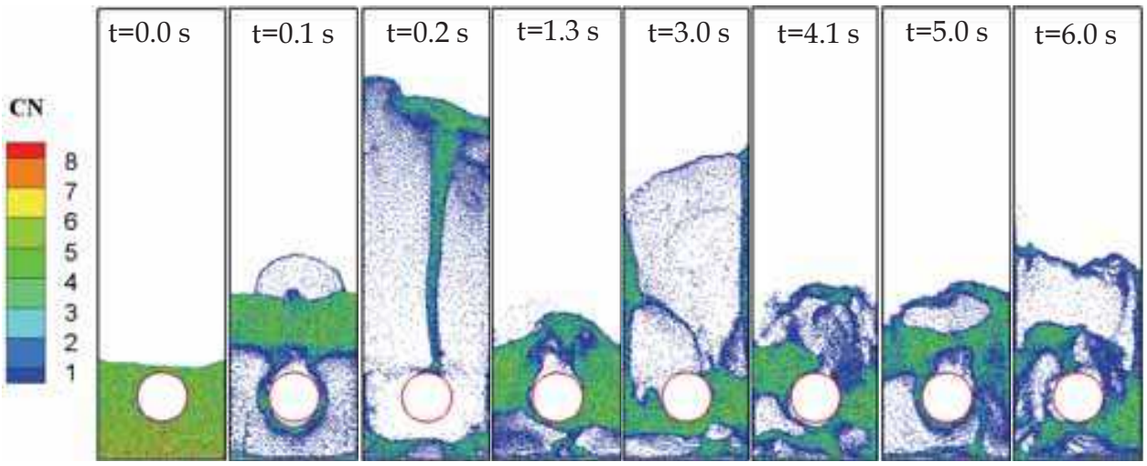

Fig. 11. Snapshots of solid flow pattern colored by coordination number of individual particles when u_{exc} = 0.50 m/s (Hou et al., 2010a).

The tube exchanges heat with its surrounding particles and fluid. The local HTC has a distribution closely related to these observed flow patterns. The distribution and magnitude of HTC are two factors commonly used to describe the heat transfer in such a system (Botterill et al., 1984; Schmidt & Renz, 2005; Wong & Seville, 2006). The effect of the gas velocity and the tube position are examined, showing consistent results with those reported in the literature (Botterill et al., 1984; Kim et al., 2003; Wong & Seville, 2006) (Fig. 12). The

local HTC is high at sides of the tube around 90° and 270° while it is low at the upstream and downstream of the tube around 0° and 180°. With the increase of gas velocity, the local HTC increases first and then decreases (Fig. 12a). The local HTC is also affected by tube positions, and increases with the increase of tube level within the bed static height as shown in Fig. 12b.

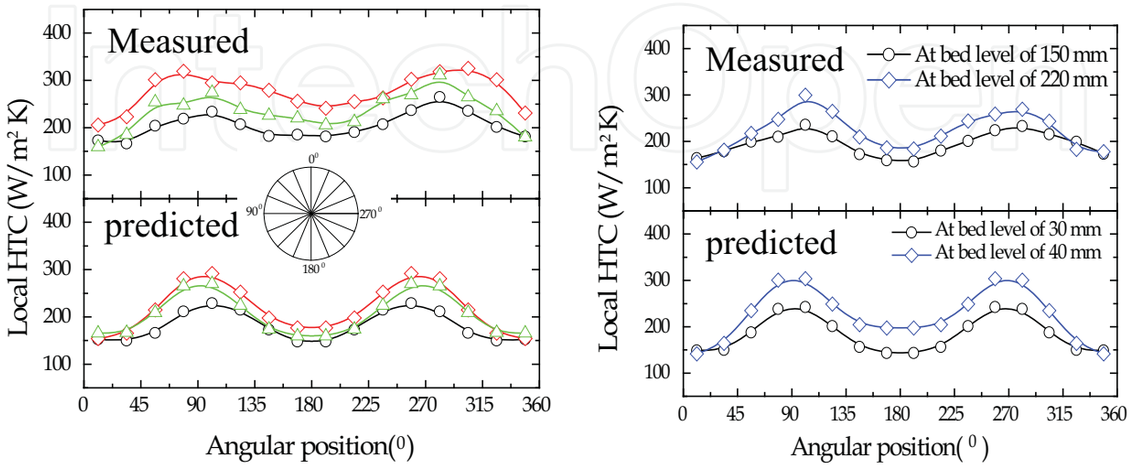

Fig. 12. Comparison of local HTCs between the predicted (Hou et al., 2010a) and the measured (Wong & Seville, 2006): (a) local HTC distribution at different excess gas velocities (u_{exc}) (○, 0.08 m/s; ◊, 0.50 m/s; and Δ, 0.80 m/s); and (b) local HTC with different tube positions when u_{exc} = 0.20 m/s.

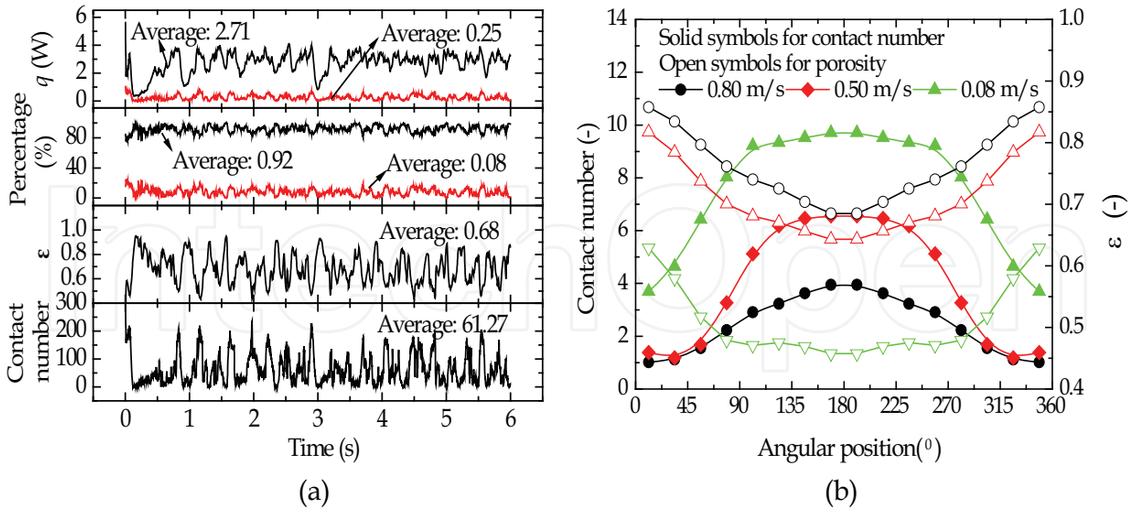

Fig. 13. (a) Overall convective and conductive heat fluxes (q) and their percentages (—, convection; ⋯, conduction), overall contact number (CN) and overall porosity (ε) as a function of time, where u_{exc} = 0.40 m/s (the overall heat flux and CN are the sum of the corresponding values of each section and the overall porosity are the averaged value of all the sections), and (b) local porosity and CN with different u_{exc} (Hou et al., 2010a).

The heat is mainly transferred through convection between gas and particles and between gas and the tube, and conduction among particles and between particles and the tube at low temperature. As an example, Fig. 13a shows the total heat fluxes through convection and conduction (the radiative heat flux is quite small at low temperatures and is not discussed here). The convective and conductive heat fluxes vary temporally. Their percentages show that the convective heat transfer is dominant with a percentage over 90%. They are closely related to the microstructure around the tube, which can be indexed by the average porosity around the tube and by the contact number (CN) between the tube and the particles. The porosity and CN vary temporally depending on the complicated interactions between the particles and the tube and between the particles and fluid, which determine the flow pattern. Generally, a region with a larger CN corresponds to a defluidized region with a smaller porosity in the vicinity of the tube. Otherwise, it corresponds to a passing bubble where the porosity is larger and the CN is smaller. Fig. 13b further shows the distributuion of local porosity and CN. It can be seen that local porosity is larger in downstream sections and lower in upstream sections while local CN has an opposite distribution.

The heat transfer between an immersed tube and a fluidized bed depends on many factors, such as the contacts of particles with the tube, porosity and gas flow around the tube. These factors are affected by many variables related to operational conditions. Gas velocity is one of the most important parameters in affecting the heat transfer, which can be seen in Fig. 12. With the increase of u_{exc} from 0.08 to 0.50 m/s, the overall heat transfer coefficient increases. However, when the u_{exc} is further increased from 0.50 to 0.80 m/s, the heat transfer coefficient decreases. The effect of particle thermal conductivity k_p on the local HTC was also examined and shown in Fig. 14a (Hou et al., 2010a). The local HTC increases with the increase of k_p from 1.10 to 100 W/(m·K). However, such an increase is not significant for k_p from 100 to 300 W/(m·K). The variations of percentages of different heat transfer modes with k_p is further shown in Fig. 14b. When k_p is lower than 100 W/(m·K), the conductive heat transfer increases with the increase of k_p while the convective heat transfer decreases. Further increase of k_p has no significant effects.

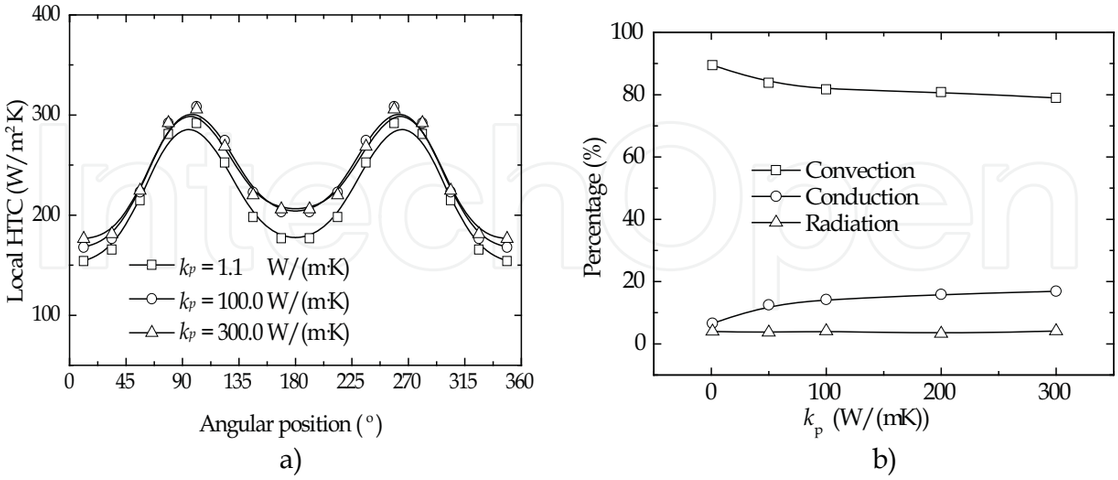

Fig. 14. Effect of k_p on: (a), local HTC; and (b), percentages of different heat fluxes; where u_{exc} = 0.50 m/s (Hou et al., 2010a).

The heat transfer by radiation is important in the considered system because the increase of environmental temperature of the tube, and its significance has already been pointed out in

the literature (see, for example, Mathur & Saxena, 1987; Chen et al., 2005). The effect of the tube temperature (T_s) on heat transfer characteristic was investigated in terms of the local HTC distribution and the heat fluxes by different heat transfer modes (Hou et al., 2010a). Fig. 15a shows that the local HTC increase with the increase of T_s. The increased trend of HTC agrees well with the results of the experiments (Botterill et al., 1984). The increase of gas thermal conductivity with temperature is one of the main reasons for the increase of HTC (Zhou et al., 2009). This manifests the importance of using the temperature related correlations of fluid properties. Variations of the heat fluxes with tube temperature T_s are shown in Fig. 15b. The conductive heat flux changes insignificantly. The convective heat flux increases linearly while the radiative heat fluxes increases exponentially with the increase of the T_s. Because of the increase of T_s, the difference between the environmental temperature (T_e) and the bed temperature (T_b) increases. The radiative heat flux increases more quickly than the convective heat flux according to the fourth power law of the temperature difference. The radiative heat flux becomes larger than that of conductive heat flux around T_s = 300°C and then, larger than that of the convective heat flux around T_s = 1200°C. These show that the radiation is an important heat transfer mode with high tube temperatures.

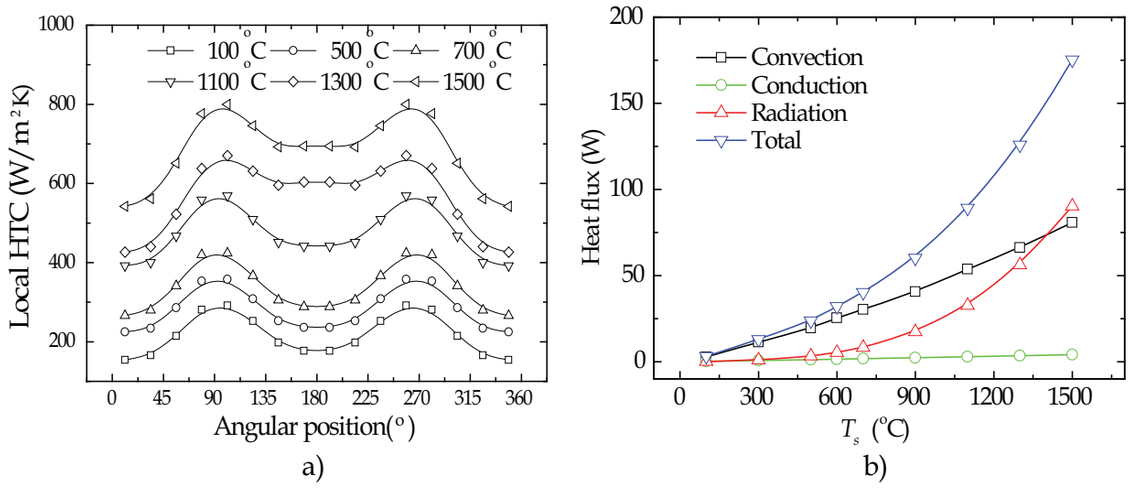

Fig. 15. Heat transfer behaviour at high tube temperatures: (a), variations of local HTC with different T_s, where u_{exc} = 0.50 m/s; and (b), convective, conductive, radiative and total heat fluxes as a function of T_s, where u_{exc} = 0.50 m/s (Hou et al., 2010a).

4. Conclusions

The DPS-CFD approach, originally applied to study the particle-fluid flow, has been extended to study the heat transfer in packed and bubbling fluidized beds at a particle scale. The proposed model is, either qualitatively or quantitatively depending on the observations in the literature, validated by comparing the predicted and measured results under different conditions. Three basic heat transfer modes (particle-fluid convection, particle conduction and radiation) are considered in the present model, and their contributions to the total heat transfer in a fixed or fluidized bed can be quantified and analyzed. The examples presented demonstrate that the DPS-CFD approach is very promising in quantifying the role of various heat transfer mechanisms in packed/fluidized beds, which is useful to the optimal design and control of fluid bed ractors.

5. References

Agarwal, P.K. (1991). Transport phenomena in multi-particle systems-IV. Heat transfer to a large freely moving particle in gas fluidized bed of smaller particles. *Chem. Eng. Sci.*, 46, 1115-1127

Anderson, T.B. & Jackson, R. (1967). Fluid mechanical description of fluidized beds-equations of motion. *Ind. Eng. Chem. Fund.*, 6, 527-539,0196-4313.

Argento, C. & Bouvard, D. (1996). Modeling the effective thermal conductivity of random packing of spheres through densification. *Int. J. Heat Mass Transfer*, 39, 1343-1350

Avedesia, M.M. & Davidson, J.F. (1973). Combustion of carbon particles in a fluidized-bed. *Trans. Inst. Chem. Eng.*, 51, 121-131,0046-9858.

Baskakov, A.P., Filippovskii, N.F., Munts, V.A. & Ashikhmin, A.A. (1987). Temperature of particles heated in a fluidized bed of inert material. *J. Eng. Phys.*, 52, 574-578,00220841.

Batchelor, G.K. & O'Brien, R.W. (1977). Thermal or electrical conduction through a granular material. *Proc. R. Soc. London, A*, 355, 313-333

Botterill, J.S.M. (1975). *Fluid-bed heat transfer*, Academic Press London, New York.

Botterill, J.S.M., Teoman, Y. & Yuregir, K.R. (1982). Minimum fluidization velocity at high-temperatures-comment. *Ind. Eng. Chem. Process Des. Dev.*, 21, 784-785,0196-4305.

Botterill, J.S.M., Teoman, Y. & Yuregir, K.R. (1984). Factors affecting heat transfer between gas-fluidized beds and immersed surfaces. *Powder Technol.*, 39, 177-189,0032-5910.

Chandran, R. & Chen, J.C. (1982). Bed-surface contact dynamics for horizontal tubes in fluidized beds. *AIChE J.*, 28, 907-914,0001-1541.

Chen, J.C. & Chen, K.L. (1981). Analysis of simultaneous radiative and conductive heat-transfer in fluidized-beds. *Chem. Eng. Commun.*, 9, 255-271,0098-6445.

Chen, J.C. (1998). Heat Transfer in Fluidized Beds. In: *Fluidization, Solids Handling, and Processing*, Y. Wen-Ching (Editor), pp. 153-208, William Andrew Publishing, 978-0-81-551427-5, Westwood, NJ.

Chen, J.C. (2003). Surface contact - Its significance for multiphase heat transfer: Diverse examples. *J. Heat Transfer-Trans. ASME*, 125, 549-566,0022-1481.

Chen, J.C., Grace, J.R. & Golriz, M.R. (2005). Heat transfer in fluidized beds: design methods. *Powder Technol.*, 150, 123-132

Cheng, G.J., Yu, A.B. & Zulli, P. (1999). Evaluation of effective thermal conductivity from the structure of a packed bed. *Chem. Eng. Sci.*, 54, 4199-4209

Cheng, G.J. (2003). Structural evaluation of the effective thermal conductivity of packed beds, the University of New South Wales.

Chung, T.Y. & Welty, J.R. (1989). Tube array heat transfer in fluidized beds- A study of particle size effects. *AIChE J.*, 35, 1170-1176,0001-1541.

Collier, A.P., Hayhurst, A.N., Richardson, J.L. & Scott, S.A. (2004). The heat transfer coefficient between a particle and a bed (packed or fluidised) of much larger particles. *Chem. Eng. Sci.*, 59, 4613-4620

Crane, R.A. & Vachon, R.I. (1977). A prediction of the bounds on the effective thermal conductivity of granular materials. *Int. J. Heat Mass Transfer*, 20, 711-723,0017-9310.

Cundall, P.A. & Strack, O.D.L. (1979). A discrete numerical-model for granular assemblies. *Geotechnique*, 29, 47-65,0016-8505.

Delvosalle, C. & Vanderschuren, J. (1985). Gas-to-particle and particle-to-particle heat transfer in fluidized beds of large particles. *Chem. Eng. Sci.*, 40, 769-779

Di Felice, R. (1994). The voidage function for fluid-particle interaction systems. *Int. J. Multiphase Flow*, 20, 153-159

Di Maio, F.P., Di Renzo, A. & Trevisan, D. (2009). Comparison of heat transfer models in DEM-CFD simulations of fluidized beds with an immersed probe. *Powder Technol.*, 193, 257-265,0032-5910.

Dong, X.F., Yu, A.B., Yagi, J.I. & Zulli, P. (2007). Modelling of multiphase flow in a blast furnace: Recent developments and future work. *ISIJ Int.*, 47, 1553-1570,0915-1559.

Enwald, H., Peirano, E. & Almstedt, A.E. (1996). Eulerian two-phase flow theory applied to fluidization. *Int. J. Multiphase Flow*, 22, 21-66

Ergun, S. (1952). Fluid flow through packed columns. *Chem. Eng. Prog.*, 48, 89-94,0360-7275.

Feng, Y.Q. & Yu, A.B. (2004). Assessment of model formulations in the discrete particle simulation of gas-solid flow. *Ind. Eng. Chem. Res.*, 43, 8378-8390,0888-5885.

Feng, Y.Q., Xu, B.H., Zhang, S.J., Yu, A.B. & Zulli, P. (2004). Discrete particle simulation of gas fluidization of particle mixtures. *AIChE J.*, 50, 1713-1728,1547-5905.

Feng, Y.Q. & Yu, A.B. (2007). Microdynamic modelling and analysis of the mixing and segregation of binary mixtures of particles in gas fluidization. *Chem. Eng. Sci.*, 62, 256-268,0009-2509.

Feng, Y.Q. & Yu, A.B. (2010). Effect of bed thickness on segregation behaviour of particle mixtures in a gas fluidized bed. *Ind. Eng. Chem. Res.*, 49, 3459–3468

Feng, Y.T., Han, K., Li, C.F. & Owen, D.R.J. (2008). Discrete thermal element modelling of heat conduction in particle systems: Basic formulations. *J. Comput. Phys.*, 227, 5072-5089,0021-9991.

Fjellerup, J., Henriksen, U., Jensen, A.D., Jensen, P.A. & Glarborg, P. (2003). Heat transfer in a fixed bed of straw char. *Energy Fuels*, 17, 1251-1258,0887-0624.

Flamant, G. & Arnaud, G. (1984). Analysis and theoretical study of high-temperature heat transfer between a wall and a fluidized bed. *Int. J. Heat Mass Transfer*, 27, 1725-1735

Flamant, G., Fatah, N. & Flitris, Y. (1992). Wall-to-bed heat transfer in gas--solid fluidized beds: Prediction of heat transfer regimes. *Powder Technol.*, 69, 223-230

Fountain, J.A. & West, E.A. (1970). Thermal conductivity of particulate basalt as a function of density in simulated lunar and martian environments. *J. Geophys. Res.*, 75, 4063-&,0148-0227.

Gidaspow, D. (1994). *Multiphase Flow and Fluidization*, Academic Press, San Diego.

Glass, D.H. & Harrison, D. (1964). Flow patterns near a solid obstacle in a fluidized bed. *Chem. Eng. Sci.*, 19, 1001-1002,0009-2509.

Gorring, R.L. & Churchill, S.W. (1961). Thermal conductivity of heterogeneous materials. *Chem. Eng. Prog.*, 57, 53-59

Holman, J.P. (1981). *Heat Transfer*, McGraw-Hill Company, 978-0070295988, New York.

Hou, Q.F., Zhou, Z.Y. & Yu, A.B. (2010a). Computational study of heat transfer in bubbling fluidized beds with a horizontal tube. AIChE J., submitted

Hou, Q.F., Zhou, Z.Y. & Yu, A.B. (2010b). Investigation of heat transfer in bubbling fluidization with an immersed tube. In: *6th International Symposium on Multiphase Flow, Heat Mass Transfer and Energy Conversion*, L.J. Guo, D.D. Joseph, Y. Matsumoto, M. Sommerfeld and Y.S. Wang (Editors), pp. 355-360, Amer Inst Physics, 978-0-7354-0744-2, Melville.

Ishii, M. (1975). *Thermo-fluid dynamic theory of two-phase flow*, Eyrolles, Paris.

Kaneko, Y., Shiojima, T. & Horio, M. (1999). DEM simulation of fluidized beds for gas-phase olefin polymerization. *Chem. Eng. Sci.*, 54, 5809-5821,0009-2509.

Kannuluik, W.G. & Martin, L.H. (1933). Conduction of heat in powders. *Proc. R. Soc. London, A-Containing Papers of a Mathematical and Physical Character*, 141, 144-158,0950-1207.

Khraisha, Y.H. (2002). Thermal conductivity of oil shale particles in a packed bed. *Energy Sources*, 24, 613-623,0090-8312.

Kim, S.W., Ahn, J.Y., Kim, S.D. & Lee, D.H. (2003). Heat transfer and bubble characteristics in a fluidized bed with immersed horizontal tube bundle. *Int. J. Heat Mass Transfer*, 46, 399-409,0017-9310.

Kobayashi, M., Maekwa, H., Nakamura, H. & Kondou, Y. (1991). Calculation of the mean thermal conductivity of heterogenious solid mixture with the Voronoi-Polyhedron element method. *Trans. Japan Soc. Mech. Eng. B*, 57, 1795-1801,03875016.

Krupiczka, R. (1967). Analysis of thermal conductivity in granular materials. *Int. Chem. Eng.*, 7, 122-144

Kunii, D. & Levenspiel, O. (1991). *Fluidization Engineering*, Butterworth-Heinemann, 978-0-409-90233-4, Boston.

Langston, P.A., Tuzun, U. & Heyes, D.M. (1994). Continuous potential discrete particle simulations of stress and velocity fields in hoppers: transition from fluid to granular flow. *Chem. Eng. Sci.*, 49, 1259-1275

Langston, P.A., Tuzun, U. & Heyes, D.M. (1995). Discrete Element Simulation of Internal-Stress and Flow-Fields in Funnel Flow Hoppers. *Powder Technol.*, 85, 153-169,0032-5910.

Launder, B.E. & Spalding, D.B. (1974). The numerical computation of turbulent flows. *Comput. Methods Appl. Mech. Eng.*, 3, 269-289

Li, J.T. & Mason, D.J. (2000). A computational investigation of transient heat transfer in pneumatic transport of granular particles. *Powder Technol.*, 112, 273-282,0032-5910.

Li, J.T. & Mason, D.J. (2002). Application of the discrete element modelling in air drying of particulate solids. *Drying Technol.*, 20, 255-282,0737-3937.

Masoumifard, N., Mostoufi, N., Hamidi, A.-A. & Sotudeh-Gharebagh, R. (2008). Investigation of heat transfer between a horizontal tube and gas-solid fluidized bed. *Int. J. Heat Fluid Flow*, 29, 1504-1511

Mathur, A. & Saxena, S.C. (1987). Total and radiative heat transfer to an immersed surface in a gas-fluidized bed. *AIChE J.*, 33, 1124-1135,0001-1541.

Mickley, H.S. & Fairbanks, D.F. (1955). Mechanism of heat transfer to fluidized beds. *AIChE J.*, 1, 374-384,0001-1541.

Molerus, O. & Wirth, K.E. (1997). *Heat transfer in fluidized beds*, Chapman and Hall, 978-0-412-60800-1, London.

Moreira, M.F.P., Thomeo, J.C. & Freire, J.T. (2005). Analysis of the heat transfer in a packed bed with cocurrent gas-liquid upflow. *Ind. Eng. Chem. Res.*, 44, 4142-4146,0888-5885.

Oka, S.N. (2004). *Fluidized bed combustion*, Marcel Dekker, Inc., New York.

Omori, Y. (1987). *Blast Furnace Phenomena and Modelling*, Elsevier Applied Science, 978-1-85166-057-5, London.

Parmar, M.S. & Hayhurst, A.N. (2002). The heat transfer coefficient for a freely moving sphere in a bubbling fluidised bed. *Chem. Eng. Sci.*, 57, 3485-3494

Patankar, S.V. (1980). *Numerical heat transfer and fluid flow*, Hemisphere, 978-0891165224, New York.

Pattipati, R.R. & Wen, C.Y. (1982). Minimum fluidization velocity at high-temperatures-response. *Ind. Eng. Chem. Process Des. Dev.*, 21, 785-786,0196-4305.

Peters, B. (2002). Measurements and application of a discrete particle model (DPM) to simulate combustion of a packed bed of individual fuel particles. *Combust. Flame*, 131, 132-146,0010-2180.

Preston, F.W. (1957). Mechanism of heat transfer in unconsolidated porous medi at low flow rates, Pennsylvania.

Prins, W., Draijer, W. & van Swaaij, W.P.M. (1985). Heat transfer to immersed spheres fixed or freely moving in a gas-fluidized bed, 20th Proceedings of the International Centre for Heat and Mass Transfer. Heat and mass transfer in fixed and fluidized beds. Washington: Hemisphere, pp. 317-331.

Rong, D.G. & Horio, M. (1999). DEM simulation of char combustion in a fluidized bed, Second International Conference on CFD in the Minerals and Process Industries,pp. 65-70, CD-ROM.

Rong, D.G., Mikami, T. & Horio, M. (1999). Particle and bubble movements around tubes immersed in fluidized beds - a numerical study. *Chem. Eng. Sci.*, 54, 5737-5754,0009-2509.

Schmidt, A. & Renz, U. (2005). Numerical prediction of heat transfer between a bubbling fluidized bed and an immersed tube bundle. *Heat Mass Transfer*, 41, 257-270,0947-7411.

Schumann, T.E.W. & Voss, V. (1934). Heat flow through granulated material. *Fuel*, 13, 249-256

Scott, S.A., Davidson, J.F., Dennis, J.S. & Hayhurst, A.N. (2004). Heat transfer to a single sphere immersed in beds of particles supplied by gas at rates above and below minimum fluidization. *Ind. Eng. Chem. Res.*, 43, 5632-5644,0888-5885.

Siu, W.W.M. & Lee, S.H.K. (2004). Transient temperature computation of spheres in three-dimensional random packings. *Int. J. Heat Mass Transfer*, 47, 887-898,0017-9310.

Sun, J. & Chen, M.M. (1988). A theoretical analysis of heat transfer due to particle impact. *Int. J. Heat Mass Transfer*, 31, 969-975

Tsuji, Y., Tanaka, T. & Ishida, T. (1992). Lagrangian numerical simulation of plug flow of cohesionless particles in a horizontal pipe. *Powder Technol.*, 71, 239-250

Vargas, W.L. & McCarthy, J.J. (2001). Heat conduction in granular materials. *AIChE J.*, 47, 1052-1059,1547-5905.

Vargas, W.L. & McCarthy, J.J. (2002a). Conductivity of granular media with stagnant interstitial fluids via thermal particle dynamics simulation. *Int. J. Heat Mass Transfer*, 45, 4847-4856,0017-9310.

Vargas, W.L. & McCarthy, J.J. (2002b). Stress effects on the conductivity of particulate beds. *Chem. Eng. Sci.*, 57, 3119-3131,0009-2509.

Verschoor, H. & Schuit, G. (1951). Heat transfer to fluids flowing through a bed of granular solids. *Appl. Sci. Res.*, 2, 97-119,0003-6994.

Waddams, A.L. (1944). The flow of heat through granular material. *J. Soc. Chem. Ind.*, 63, 337-340

Wakao, N. & Kaguei, S. (1982). *Heat and Mass Transfer in Packed Beds*, Gordon and Breach Science Publishers, New York.

Wen, C.Y. & Yu, Y.H. (1966). Mechanics of fluidization,pp. 100-111,

Wilhelm, R.H., Johnson, W.C., Wynkoop, R. & Collier, D.W. (1948). Reaction rate, heat transfer, and temperature distribution in fixed-bed catalytic converters - solution by electrical network. *Chem. Eng. Prog.*, 44, 105-116,0360-7275.

Wong, Y.S. & Seville, J.P.K. (2006). Single-particle motion and heat transfer in fluidized beds. *AIChE J.*, 52, 4099-4109,0001-1541.

Xu, B.H. & Yu, A.B. (1997). Numerical simulation of the gas-solid flow in a fluidized bed by combining discrete particle method with computational fluid dynamics. *Chem. Eng. Sci.*, 52, 2785-2809

Xu, B.H. & Yu, A.B. (1998). Comments on the paper "Numerical simulation of the gas-solid flow in a fluidized bed by combining discrete particle method with computational fluid dynamics" - Reply. *Chem. Eng. Sci.*, 53, 2646-2647,0009-2509.

Xu, B.H., Yu, A.B., Chew, S.J. & Zulli, P. (2000). Numerical simulation of the gas-solid flow in a bed with lateral gas blasting. *Powder Technol.*, 109, 13-26

Yagi, S. & Kunii, D. (1957). Studies on effective thermal conductivities in packed beds. *AIChE J.*, 3, 373-381,0001-1541.

Yang, R.Y., Zou, R.P. & Yu, A.B. (2000). Computer simulation of the packing of fine particles. *Phys. Rev. E*, 62, 3900-3908

Yu, A.B. & Xu, B.H. (2003). Particle-scale modelling of gas-solid flow in fluidisation. *J. Chem. Technol. Biotechnol.*, 78, 111-121,0268-2575.

Zehner, P. & Schlünder, E.U. (1970). Thermal conductivity of packed beds (in German). *Chem. Ing. Tech.*, 42, 933-941,1522-2640.

Zhao, Y.Z., Jiang, M.Q., Liu, Y.L. & Zheng, J.Y. (2009). Particle-scale simulation of the flow and heat transfer behaviors in fluidized bed with immersed tube. *AIChE J.*, 55, 3109-3124,1547-5905.

Zhou, H.S., Flamant, G., Gauthier, D. & Flitris, Y. (2003). Simulation of coal combustion in a bubbling fluidized bed by distinct element method. *Chem. Eng. Res. Des.*, 81, 1144-1149,0263-8762.

Zhou, H.S., Flamant, G. & Gauthier, D. (2004). DEM-LES simulation of coal combustion in a bubbling fluidized bed Part II: coal combustion at the particle level. *Chem. Eng. Sci.*, 59, 4205-4215,0009-2509.

Zhou, J.H., Yu, A.B. & Horio, M. (2008). Finite element modeling of the transient heat conduction between colliding particles. *Chem. Eng. J.*, 139, 510-516,1385-8947.

Zhou, Y.C., Wright, B.D., Yang, R.Y., Xu, B.H. & Yu, A.B. (1999). Rolling friction in the dynamic simulation of sandpile formation. *Physica A*, 269, 536-553

Zhou, Z.Y., Yu, A.B. & Zulli, P. (2009). Particle scale study of heat transfer in packed and bubbling fluidized beds. *AIChE J.*, 55, 868-884,1547-5905.

Zhou, Z.Y., Yu, A.B. & Zulli, P. (2010a). A new computational method for studying heat transfer in fluid bed reactors. *Powder Technol.*, 197, 102-110,0032-5910.

Zhou, Z.Y., Kuang, S.B., Chu, K.W. & Yu, A.B. (2010b). Discrete particle simulation of particle-fluid flow: Model formulations and their applicability. *J. Fluid Mech.*, 661, 482-510.

Zhu, H.P., Zhou, Z.Y., Yang, R.Y. & Yu, A.B. (2007). Discrete particle simulation of particulate systems: Theoretical developments. *Chem. Eng. Sci.*, 62, 3378-3396.

Zhu, H.P., Zhou, Z.Y., Yang, R.Y. & Yu, A.B. (2008). Discrete particle simulation of particulate systems: A review of major applications and findings. *Chem. Eng. Sci.*, 63, 5728-5770.

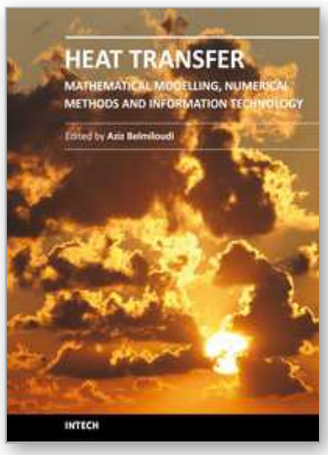

Heat Transfer - Mathematical Modelling, Numerical Methods and Information Technology

Edited by Prof. Aziz Belmiloudi

ISBN 978-953-307-550-1
Hard cover, 642 pages
Publisher InTech
Published online 14, February, 2011
Published in print edition February, 2011

Over the past few decades there has been a prolific increase in research and development in area of heat transfer, heat exchangers and their associated technologies. This book is a collection of current research in the above mentioned areas and describes modelling, numerical methods, simulation and information technology with modern ideas and methods to analyse and enhance heat transfer for single and multiphase systems. The topics considered include various basic concepts of heat transfer, the fundamental modes of heat transfer (namely conduction, convection and radiation), thermophysical properties, computational methodologies, control, stabilization and optimization problems, condensation, boiling and freezing, with many real-world problems and important modern applications. The book is divided in four sections : "Inverse, Stabilization and Optimization Problems", "Numerical Methods and Calculations", "Heat Transfer in Mini/Micro Systems", "Energy Transfer and Solid Materials", and each section discusses various issues, methods and applications in accordance with the subjects. The combination of fundamental approach with many important practical applications of current interest will make this book of interest to researchers, scientists, engineers and graduate students in many disciplines, who make use of mathematical modelling, inverse problems, implementation of recently developed numerical methods in this multidisciplinary field as well as to experimental and theoretical researchers in the field of heat and mass transfer.

INTECH
open science | open minds

InTech Europe
University Campus STeP Ri
Slavka Krautzeka 83/A
51000 Rijeka, Croatia
Phone: +385 (51) 770 447

InTech China
Unit 405, Office Block, Hotel Equatorial Shanghai
No.65, Yan An Road (West), Shanghai, 200040, China
中国上海市延安西路65号上海国际贵都大饭店办公楼405单元
Phone: +86-21-62489820

Fax: +385 (51) 686 166
www.intechopen.com

Fax: +86-21-62489821

IntechOpen